Wind Stress and Heat Flux over the Ocean in Gale Force Winds[1]

STUART D. SMITH

Bedford Institute of Oceanography, P.O. Box 1006, Dartmouth, Nova Scotia, Canada B2Y 4A2

(Manuscript received 15 June 1979, in final form 15 January 1980)

ABSTRACT

An offshore stable platform has been instrumented with wind turbulence, temperature and wave height sensors. Data from this platform have been analyzed by the eddy correlation method to obtain wind stress and heat flux at wind speeds from 6 to 22 m s^{-1} in a deep-water wave regime, significantly extending the range of available measurements. The sea surface drag coefficient increases gradually with increasing wind speed.

Sensible heat fluxes have been observed over a much wider range than previously available. Heat flux coefficients are higher in unstable than stable conditions, but are not seen to increase with increasing wind speed.

1. Introduction

Wind stress and sensible heat exchange at the sea surface play major roles in the movement and the formation of water masses and also of air masses. The wind stress and heat flux may be obtained from measurements of winds and temperatures by several methods, such as the eddy correlation, the profile and the dissipation methods (Busch, 1977; Kraus, 1972). In this paper we shall use the eddy correlation method, which is the most direct. This requires that we measure the downwind and vertical wind fluctuations u_1 and u_3, respectively, and the temperature fluctuations t at a fixed point. In the surface layer the shearing stress

$$\tau = -\overline{\rho u_1 u_3} \approx -\overline{\rho u_1 u_3} \tag{1}$$

is nearly independent of height and the drag coefficient is

$$C_{10} = \frac{\tau}{\rho U_{10}^2} = \frac{-\overline{u_1 u_3}}{U_{10}^2}, \tag{2}$$

where the subscript 10 denotes a reference height $z = 10$ m.

The heat flux is

$$H = \overline{\rho C_p t u_3} \approx \rho C_p \overline{t u_3}, \tag{3}$$

where ρ is the density and C_p the specific heat of air, and the heat flux coefficient, also called a Stanton number, is

$$C_T = \frac{H}{\rho C_p (T_s - T_a) U_{10}} = \frac{\overline{t u_3}}{(T_s - T_a) U_{10}}, \tag{4}$$

where T_s is the sea water "bucket" temperature in the wave-mixed layer and T_a the mean air temperature at the 10 m reference height. The overbar denotes a time average over a period long enough to form stable averages of turbulent properties and short enough for mean conditions to be steady, which we shall usually take to be ~40 min.

a. Review of sea surface drag coefficients

The drag coefficient is a function of surface roughness and of atmospheric stability (z/L), where z is the reference height and the Monin-Obukhov length is

$$L = -T_a u_*^3 / g K \overline{t u_3}, \tag{5}$$

in which we take gravity to be $g = 9.8$ m s^{-2}, the von Kármán constant to be $K = 0.4$, and T_a to be absolute temperature. The friction velocity is $u_* = (-\overline{u_1 u_3})^{1/2}$. More generally the stability and the Monin-Obukhov length L also depend on the rate of evaporation (e.g., Pond *et al.*, 1971). The evaporation term is relatively small for the fall and winter data to be presented here, but can become dominant over tropical oceans.

1) THE EFFECT OF STABILITY

For particular values of u_* and U a few centimeters above the surface the mean wind gradient is steeper in stable than in unstable conditions. The wind profile over land has been extensively studied and in a review Dyer (1974) recommends the empirical formulas for the profile gradient function

$$\phi_m = \begin{cases} 1 + 5z/L, & z/L > 0, \quad (6) \\ [1 - 16(z/L)]^{-1/4}, & z/L < 0, \quad (7) \end{cases}$$

[1] This project has been identified as a Canadian contribution to the Global Atmospheric Research Project (GARP).

0022-3670/80/050709-18$08.50

where the profile gradient is

$$\frac{dU}{dz} = \frac{u_*}{Kz}\,\phi_m(z/L). \tag{8}$$

Deardorff (1968) has integrated the profile gradients with height to obtain the stability-dependent wind profile and drag coefficient. Deardorff also gives equivalent results for heat flux and evaporation coefficients, using a higher rate of variation in Eq. (6) than does Dyer (1974)—the constant 5 is replaced by a value of 7 for wind speed and 11 for temperature. Kondo (1975) has plotted drag, heat flux and evaporation coefficients as functions of wind speed and sea-air temperature difference. Hsu (1974) summarizes wind stress data from a number of sources including Smith (1973, 1974b) to derive a value of 4.4 for the constant shown as 5 in Eq. (6). Although this equation is usually proposed for $z/L > 0$ he includes some data with $z/L < 0$ in his analysis.

2) The neutral drag coefficient

Over land surfaces the surface roughness and the drag coefficient in neutral stability are constant at any given location, although it can be difficult to find a homogeneous site where eddy flux or other wind stress measurements can be clearly related to a particular type of surface. Over the sea the surface roughness is determined by the waves and homogeneous conditions are easier to find. However, the sea state depends not only on the local wind speed but also on fetch, duration, water depth and surface slick conditions. Assuming that it is the shorter, steeper waves which are primarily responsible for variations in the drag coefficient and that these are usually in equilibrium with the local wind, Charnock (1955) predicted by a dimensional argument that the surface roughness height z_0 should be proportional to the stress,

$$z_0 = au_*^2/g, \tag{9}$$

in the neutral wind profile equation

$$U(z) = \frac{u_*}{K}\ln\frac{z}{z_0}, \tag{10}$$

leaving only the constant a to be determined experimentally. This results in a slightly nonlinear increase in the drag coefficient with wind speed, namely

$$C_{10} = (u_*/U)^2 = [K/\ln(gz/au_*^2)]^2, \tag{11}$$

where we customarily take $z = 10$ m as a reference height.

Flow over a smooth surface results in a thin laminar sublayer in which velocity increases linearly with height, above which the wind profile becomes

$$U/u_* = (1/K)\ln(u_*z/\nu) + 5.5, \tag{12}$$

where $\nu = 14 \times 10^{-6}$ m^2 s^{-1} is the kinematic viscosity of air (see, e.g., Businger, 1973).

The smooth surface drag coefficient increases with *decreasing* wind speed and should apply at low wind speeds wherever it is greater than that from Eq. (11).

The question of whether the neutral-stability sea surface drag coefficient is constant or increases with wind speed[2] and wave height has for years occupied a high priority (e.g., Stewart, 1961, 1967, 1974). Prior to 1975 "the observational evidence supports a constant (drag coefficient) just as well as Charnock's formula" (Businger, 1975). Garratt (1977), summarizes sea surface drag coefficients from 17 experiments (all but one based on eddy correlation and/or wind profile data) published from 1967 to 1975, and a synthesis of the results of 12 of these, judged to be the most reliable, supports the Charnock formula [Eq. (11)]. The data in this review at wind speeds above 16 m s^{-1} (from Smith and Banke, 1975) are not entirely representative of the open ocean since they are possibly influenced by a shoal area of breaking waves upwind of the sensors.

Studies of geostrophic wind departures in hurricanes indicate a linear increase of the drag coefficient with wind speeds up to 50 m s^{-1} but with very large (50–100%) possible experimental errors. Miller (1964) drew precisely the same linear variation of the drag coefficient with wind speeds to 50 m s^{-1} as the linear relation fitted by Garratt (1977) to more recent profile and eddy flux data.

Kondo *et al.* (1973) and Kondo (1975) find that the sea surface drag coefficient is related to the measured height of the waves at frequencies of a few hertz, which becomes large enough for the surface to be fully rough at a wind speed of 8 m s^{-1} and continues to grow with wind speeds up to a maximum observed speed of 14 m s^{-1}. Specialized instrumentation is required to measure these high-frequency waves with heights of millimeters to centimeters in the presence of much larger waves (meters) at frequencies around the peak of the wave spectrum.

b. Review of heat fluxes

Sensible and latent heat exchange, and radiative heat exchange at the sea surface are responsible for the formation of water and air masses of various temperatures and densities. The heat flux coefficient C_T [Eq. (4)] is expected to vary somewhat more with stability than is the drag coefficient (Deardorff, 1968) but the "neutral" heat flux coefficient is difficult to determine experimentally. Unlike momen-

[2] As pointed out by K. Hasselmann (see Smith, 1978, p. 50), the dimensionless drag coefficient should properly depend on a dimensionless velocity or Froude number $F = U/(gz)^{1/2}$ (Wu, 1969) which in the following discussions can be conveniently taken to be $F \approx U_{10}/10$ m s^{-1}.

tum, heat is not transmitted by form drag on surface waves and so the mechanism for a Charnock-type wind speed dependence is not indicated. However, waves and spray do increase the surface area and so it is plausible that the coefficient C_T might increase with wind speed.

Sensible (and latent) heat fluxes have been reviewed by Friehe and Schmitt (1976), to obtain $C_T = 0.86 \times 10^{-3}$ in stable and 0.97×10^{-3} in unstable conditions, over a range of $U_{10}(T_s - T_a) = -15$–20°C m s^{-1}. At mid and high latitudes most of the heat transport occurs at much higher values of $U_{10}(T_s - T_a)$. If Smith and Banke's (1975) data with $U_{10}(T_s - T_a)$ up to 160°C m s^{-1} are included, they dominate other values in Friehe and Schmitt's regression to give an overall value of $C_T = 1.4 \times 10^{-3}$.

Smith and Banke were not able to monitor the sea surface temperature during their high-wind data runs and so there is a possible error of ~20% in their values of $(T_s - T_a)$. Heat flux measurements at Sable Island in moderate wind conditions (e.g., Smith *et al.*, 1976) give lower values of C_T comparable to those of Friehe and Schmitt for other sites and this suggests that C_T may also increase with wind speed. Francey and Garratt (1978, 1979) found that the heat flux coefficient increased with wind speed in the same way as the drag coefficient during the AMTEX experiment, in which their island sites were generally similar to Sable Island in having shoal water upwind of the anemometers. At long fetch, measuring eddy fluxes from an aircraft flying at 100 m height, Coulman (1979) found $C_T = 1.4 \times 10^{-3}$ and detected no variation with wind speed from 5 to 11 m s^{-1}. His use of radiometric surface temperature may make T_s closer to T_a and C_T larger than in other studies with bulk water temperature.

c. *Experimental considerations*

Measurements of the neutral sea surface drag coefficient as a function of wind speed are inherently scattered because of 1) experimental errors in sensor response, and flow distortion by and motion of the supporting tower; 2) other variables which may affect the fluxes, such as sea state, depth, fetch and the presence of slicks; and 3) the use of a finite averaging period to represent long-term, steady-state conditions. With the usual experimental and statistical scatter it is difficult to resolve changes of less than 20% in the drag coefficient, and a convincing test of Charnock's relation requires a large number of measurements over a wind speed range of ~8–20 m s^{-1} for a predicted change of 60% in the drag coefficient. Similarly a large number of measurements over a wide range of conditions is needed to parameterize the heat flux.

For air-sea interaction measurements to be representative of the open sea, the chosen site must be open to a long fetch and must be in water deep enough that waves are not slowed and steepened by passage over shoals. Sensors for such an experiment must be mounted on a structure which is sufficiently slender to negligibly distort the wind flow. It must either be sufficiently rigid to impart negligible errors by its motion to the measured wind fluctuations, or else its motion must be measured and used to correct the measurements. It is the difficulty of providing such a stable platform and of maintaining sensitive measuring equipment on it which has in the past limited such measurements to moderate wind conditions.

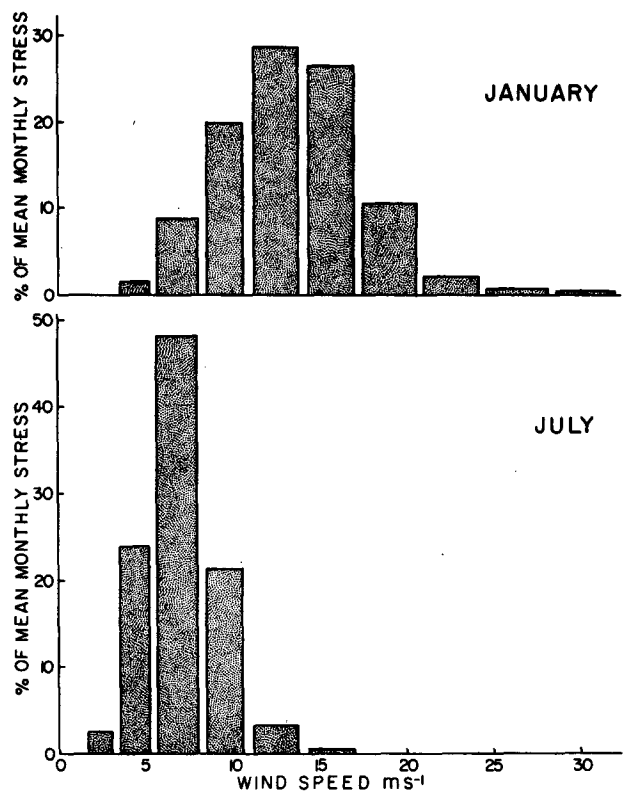

FIG. 1. Mean monthly sea surface stress distribution with wind speed for Sable Island, Nova Scotia region, January and July. Wind speed distribution from Atmospheric Environment Service, Canada, for 1957–66. Drag coefficient from Smith and Banke (1975).

d. *Purpose of experiment*

The principal motivation for undertaking the experiment to be described here has been to directly measure the sea surface drag coefficient over a wide enough range of wind speeds to determine the mean wind stress in most climates and to resolve variation of the drag coefficients with wind speed, stability and sea state.

For the Sable Island, Nova Scotia area (44°N, 60°W) in January nearly half of the mean wind stress occurs at wind speeds above 15 m s^{-1} (Fig. 1) for

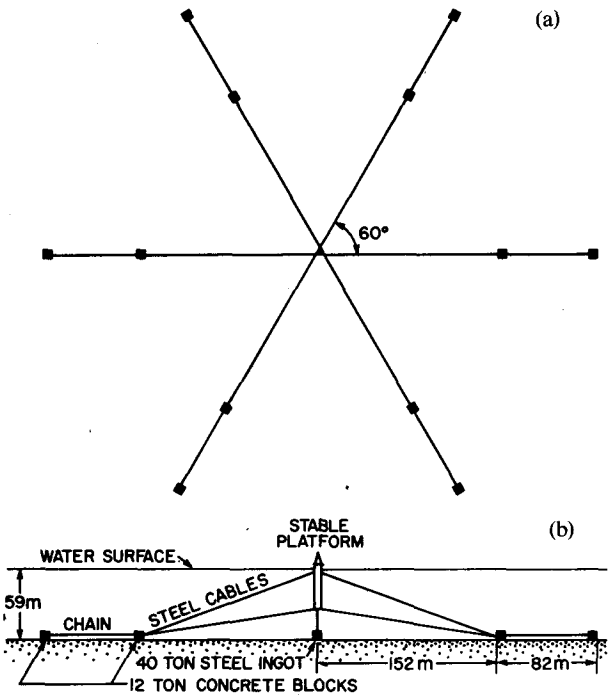

FIG. 2. Mooring of the stable platform, (a) plan, (b) elevation, with only two pairs of the concrete anchors shown.

which hardly any open-sea measurements are available, although in July storms are rare and nearly all the stress lies within the range of available data. A second major objective has been to investigate the sensible heat flux over a range of conditions representative of midlatitude climates and to find appropriate values of C_T.

This paper gives wind stress and heat flux results from the thrust anemometer and thermistor data, and their relation to parameters such as wind speed, rms wave height, and water and air temperatures.

2. The BIO stable platform experiment

a. The platform

For the present experiments a stable platform was designed to withstand a combination of 1) waves of 18 m height, peak-to-trough; 2) 45 m s^{-1} mean wind with gust factor 1.25; and 3) a current of 0.25 m s^{-1}. The structure was a floating tower or spar buoy 47 m long weighing 25.5 metric tons with displacement of 60.5 tons provided by six flotation tanks. It was held down by six diagonal anchor lines attached just below the water surface, six more diagonal lines attached at the bottom, and a single vertical line (Fig. 2). Six outer anchors consisted of two 10.9-ton concrete blocks joined by 82 m of chain, the center anchor being a 36.4-ton steel ingot. When in position, the upper tower rose 12.5 m above mean water level (Fig. 3). The platform was on location (Fig. 4) from 6 June 1976 until 17 February 1978. The water depth was 59 m, allowing 10 s waves to travel at 99% of their deep-water phase velocity (12 s waves, 96%); thus it was typically in deep-water waves. It was exposed to the full fetch of the North Atlantic Ocean for winds from the south and east, and a minimum fetch of 10 km from shore for west winds. The platform was visited during periods of calm weather to install, check or repair the instruments, but was unmanned during data-recording periods.

b. Instrumentation

A thrust anemometer (Smith, 1980) was used to sense the wind thrust vector on a perforated sphere of 3.8 cm diameter, using a three-axis spring assembly and three displacement transducers. A Bendix Aerovane anemometer provided a continuous check of thrust anemometer calibration. A micro-thermistor with a time constant of 0.03 s sensed mean air temperature and temperature fluctuations. A Nova Scotia Research Foundation resistance wire wave staff sensed surface elevation at one point, giving wave height but not direction. The performance of the stable platform was monitored by six strain gages in the six upper anchor cables, and a three-axis accelerometer.

A telemetry system (Dinn, 1973) transmitted data at 228 MHz over a 26 km range to a receiving antenna at the Bedford Institute of Oceanography (BIO). A 465 MHz radio remote control turned the system on and off, controlled amplifier gains, opened and closed a hood on the thrust anemometer and thermistor, and selected which 12 channels of data were to be transmitted.

The remote systems were powered by nine automobile batteries connected to give a reserve of 10 KW h and charged by a 25 W Aerowatt windmill generator. The power drain was 50–100 W with the system operating, but only 1.3 W in a standby (receiver only) mode when data were not required. Battery voltage was telemetered to monitor the charging system.

The BIO system was operational for a total of 184 days during the periods 7–28 October, 1976; 8 November–8 December 1976; 5–15 February 1977; 4 March–18 April 1977; 29 October–30 November 1977; and 29 December–7 February 1978. The original plan was to run from 1 October until 31 March for two seasons, but the experiment was terminated by a collapse of the moorings of the stable platform during a storm on 7 February 1978. The design wave height (18 m) was not reached, but a number of factors including ice accumulation are believed to have contributed. The structure, the telemetry system, the thrust anemometer and the windmill generator were recovered with minimal damage after their immersion.

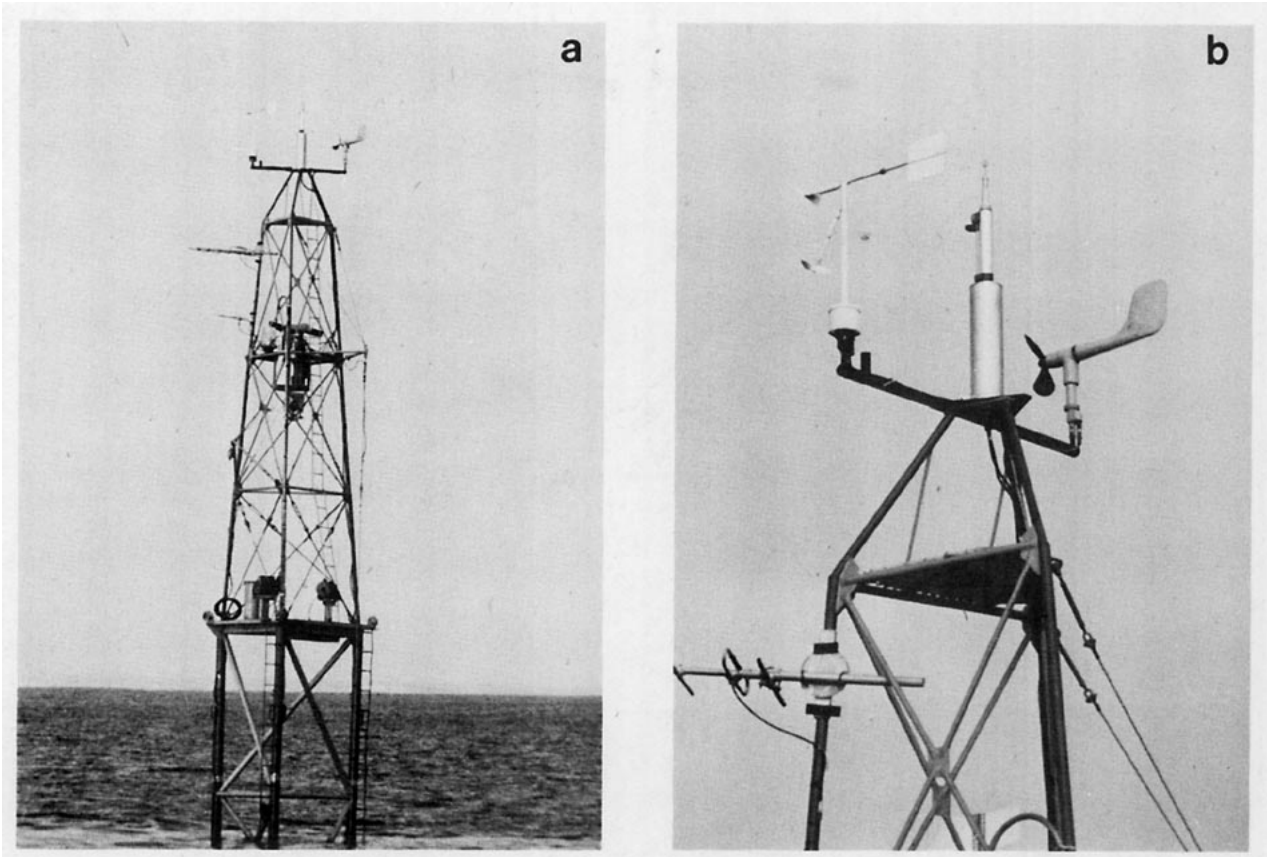

FIG. 3. The stable platform (a) and sensors (b) left to right: UBC Gill anemometer, Mk8 thrust anemometer, Bendix Aerovane anemometer.

A University of British Columbia (UBC) sensor system was used on the stable platform by Pond and Large (1978) to obtain parallel measurements of wind and temperature fluctuations during the fall and winter of 1976–77. This system also included a thermistor to measure water temperature at a depth of 5–10 m, and an on-board digital recorder. The UBC data were also telemetered occasionally using the BIO system for direct comparisons of sensor performance. During the fall and winter of 1977–78 a modified Gill propellor anemometer and the sea temperature thermistor from the UBC system were interfaced directly to the BIO telemetry system. A trial was carried out at a beach site (Smith *et al.*, 1976) to test the compatibility of the two systems.

c. Data recording

The data were recorded on magnetic tape in multiplexed FM form, in runs of ~40 min duration. Data were recorded more frequently during storm periods to cover conditions in which eddy flux measurements at sea have not been available. The records were subsequently digitized and analyzed at the BIO Computing Centre (Smith, 1974a; Dobson *et al.*, 1974).

A total of 160 runs were recorded with thrust anemometer data. Of these, three were in calm conditions and 10 were rejected because signals ran offscale, snow and ice accumulation was suspected, or electronic failures occurred. Among the remaining 147 runs, there were 27 in which the indicated lateral stress components was equal to or greater than half of the longitudinal stress component, i.e.,

$$|\overline{u_2u_3}| > -0.5\overline{u_1u_3}. \tag{13}$$

This problem will be discussed in the following section.

Results from 64 data runs with onshore winds and unlimited fetch are listed in Table 1, while Table 2 gives results for 56 runs taken during periods of offshore and alongshore winds. Preliminary results from the first season of the present experiment have been given by Smith (1978).

The tabulated wind speeds have been adjusted from the thrust anemometer height $z = 13.4$ m to a 10 m height using a neutral logarithmic profile formula [Eq. (10)]. In typical cases U_{10} is 2.5% smaller than U.

Three thrust anemometers were used during the experiment. Two of these (6.4, 8.1) agreed with the

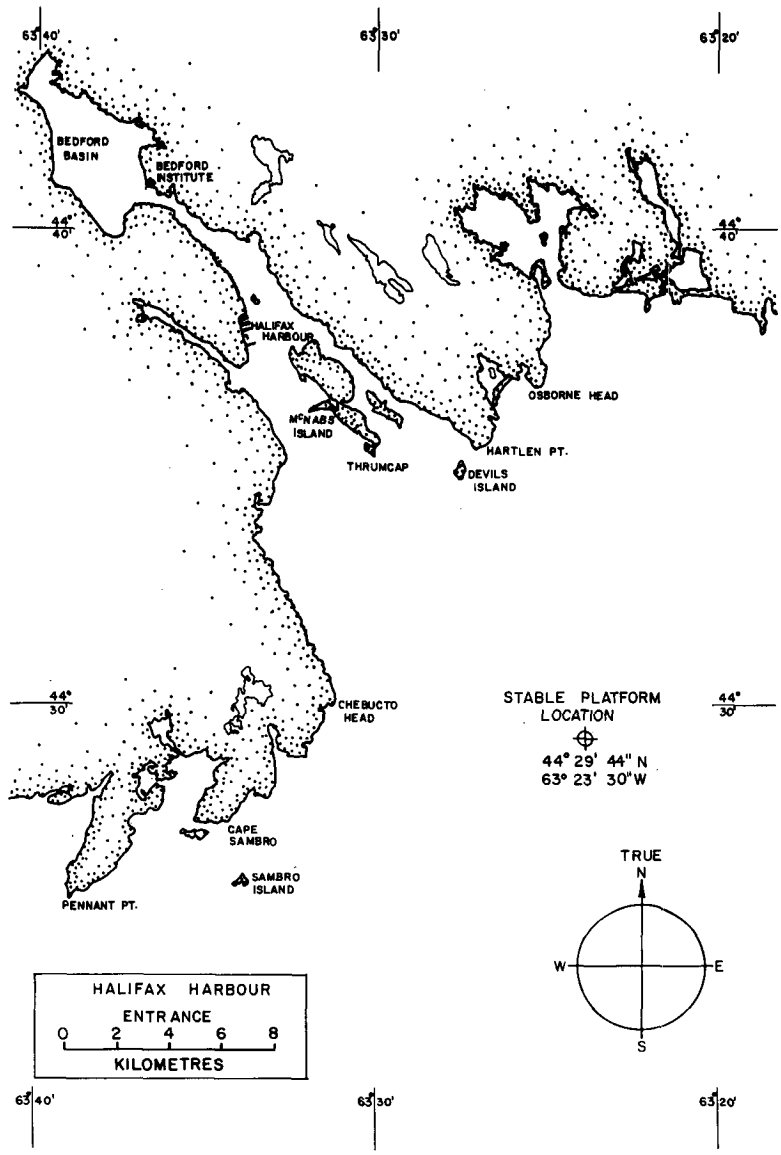

FIG. 4. Location of stable platform.

Aerovane anemometer in mean wind speed within ± 0.4 m s^{-1}. The wind tunnel calibration of the remaining thrust anemometer (6.3) used during the majority of the experiment gave wind speeds which were consistently 8% high (Fig. 5) and all the mean and fluctuating velocities from this anemometer have been reduced by 8% in Tables 1 and 2. This also gives better agreement with Gill propellor anemometer data.

Before the data were analyzed by computer, oscillograph records were examined to identify recording flaws and also departures from steady-state conditions. In a few cases data runs had to be cut short to avoid rapid changes in wind speed, direction or air temperature. As a further check, the eddy fluxes and the horizontal and vertical turbulent energy were averaged over 12.8 s intervals throughout each data run and plotted as time series, which were examined for anomalous variability.

d. Platform motion effects

During service trips on relatively calm days, the only observable motion of the platform was yaw rotation by a few degrees about the vertical axis of the platform. Although there were no rotation sensors, we expect that such motions would become larger during storm conditions.

Rotation θ about a vertical yaw axis would cause spurious horizontal crosswind fluctuations $u_2' = U \sin\theta$, while $u_1' = U(1 - \cos\theta)$ is very small for reasonable values of $\theta = 10$–$15°$. The effect on measured fluxes should therefore be minimal. Pond (1968) has shown that pitching of an anemometer support by a few degrees also causes negligible flux errors. However, if pitch and yaw motions of the platform are coupled, then much larger flux errors can result. Our data analysis procedure corrects $\overline{u_1u_3}$ for mean tilt of the tower about the x_2 axis and for cross-coupling of the x_1 and x_3 anemometer axes. Since no such corrections are applied to $\overline{u_2u_3}$, the values obtained are less reliable. Since we assume constant flux with height in the surface layer, we expect $\overline{u_2u_3}$ to be much less than $-\overline{u_1u_3}$, i.e., the stress is expected to be in the direction of the mean wind.

The mooring cables (upper and lower) were tightened uniformly during the summer of 1977. This made the yaw rotation period ~10 s, which is often near the peak of the wave spectrum. Perfectly balanced cable tensions would eliminate yaw moments associated with wave loads on the structure, and pitching moments associated with reactions to yaw motions. During the first 22 runs tabulated for the fall 1977 season (1–27 November) no cases with large $\overline{u_2u_3}$ [Eq. (13)] were encountered. During the aftermath of a storm on 27 November with the largest waves encountered up to that date, five runs with high values of $\overline{u_2u_3}$ were recorded, and only two runs with smaller values.

Similarly, during the period 7–12 October 1976 before tightening of the upper cables had been completed, three out of five thrust anemometer runs gave high values of $\overline{u_2u_3}$. The upper mooring cable tensions were adjusted on 14 October 1976, but time, weather and resources did not permit further adjustments during that storm season. A smaller proportion, 13 out of 60, of the runs taken during the fall and winter after 14 October 1976 had high values of $\overline{u_2u_3}$.

While a high value of $\overline{u_2u_3}$ does not in itself mean that the other flux values are also contaminated by platform motion, it does indicate that (i) the platform is relatively lively, (ii) the anemometer is not resolving velocity components properly, or (iii) the stress is not in the wind direction. Many of the runs with high values of $\overline{u_2u_3}$ had low values of C_{10} (11 values of $C_{10} \leq 0.65 \times 10^{-3}$ compared to only one such value in the data tabulated here). Runs with high $\overline{u_2u_3}$ [Eq. (13)] are deleted in this paper although this is not advocated as a general method for wind stress data selection.

Horizontal motion of the platform with the waves may introduce errors u_1' in the downwind velocity fluctuations which appear as a wave-frequency peak in the downwind velocity spectrum. Vertical motion is restrained to trivial values by the heavy central anchor cable, but vertical velocity errors due to pitching motions may correlate with u_1' to produce errors in the measured stress $\overline{u_1u_3}$ which result in peaks or troughs at frequencies near the peak of the wave spectrum in the stress cospectrum when plotted in the form $f\phi_{13}(f)$ vs $\log f$. Such peaks or troughs in the cospectrum, identifiable in about one-third of the present data set, have not been observed to the same extent in measurements over smaller waves (e.g., Smith, 1974b) nor at a fixed tower on a beach (Smith and Banke, 1975). Since the height of the present measurements is a smaller fraction of wavelength and wave height, a comparison with other data does not necessarily rule out the possibility of part of such peaks being real. Adjusting the cospectrum $f\phi_{13}(f)$ to cut off peaks and troughs at the wave frequency changes $\overline{u_1u_3}$ usually by only a small amount and very rarely more than 15%, and does not materially reduce the scatter in the drag coefficient. Because of irregularities normally present in the cospectrum, it was difficult to decide exactly how much of a peak or trough should be removed. The tabulated flux values have *not* been adjusted to remove cospectral peaks or troughs.

The temperature fluctuation measurement is almost unaffected by platform motions. Small wave-frequency peaks in the heat flux cospectra occurred in a few cases, but they were not large enough to affect the fluxes by more than a few percent.

3. The drag coefficient of the sea surface

a. Variation with wind speed

In addition to the 38 drag coefficients from Table 1 (long fetch) in near-neutral stability (for which $-0.1 \leq z/L \leq 0.05$), Fig. 6a shows 25 points, covering a lower wind speed range, from similar experiments with Mk6 thrust anemometers at the same site in 1968–69 (Smith, 1970, 1973). The distribution of the data with wind speed resembles the January surface stress distribution (Fig. 1). In the earlier experiments, temperature fluctuations were not measured and stability was estimated indirectly. A regression line of C_{10} on U_{10} (Fig. 6a) is

$$10^3 C_{10} = 0.61 + 0.063 U_{10} \qquad (14)$$

for wind speeds from 6 to 22 m s^{-1}. A Student's t test indicates that the increase in drag coefficient with wind speed is statistically significant well above the 99.9% level. The present result [Eq. (14)] is only 4% lower than that obtained from an earlier compilation of the author's data [Smith and Banke, 1975, Eq. (1)], much of which was taken at limited fetch or at a beach site. At a wind speed of 15 m s^{-1} the present result is 11% lower than the composite

TABLE 1. Thrust anemometer data at long fetch.

Run No.	Start time (GMT)	Date	Wind direction (deg T)	Wind speed U_{10} (m s^{-1})	Turbulence level σ_1/U	σ_2/U	σ_3/U	Drag coefficient 10^3C_{10}	rms wave height (m)	$T_s - T_a$ (°C)	Heat flux (W m^{-2})	10^3C_T	Stability z/L
					Year 1976								
6	1930	14 Oct	187	11.6	0.082	0.065	0.042	1.05	0.46	−2.6	—	—	0.072*
10	0818	21 Oct	118	18.1	0.109	0.077	0.046	1.39	0.72	−2.5	−37	0.50	0.018
11	1231	21 Oct	154	19.4	0.114	0.106	0.050	1.59	0.81	−2.4	−33	0.54	0.010
15	1511	21 Oct	175	19.8	0.110	0.092	0.061	2.52	0.90	−5.5	—	—	0.018*
16	1619	21 Oct	201	21.9	0.122	0.107	0.058	2.05	1.11	−4.6	—	—	0.017*
24	1210	2 Dec	146	8.5	0.120	0.156	0.039	0.97	0.38	0.7	15	—	−0.123
25	1343	2 Dec	158	9.5	0.089	0.075	0.038	1.21	0.35	0.0	11	—	−0.044
26	1713	2 Dec	125	11.3	0.095	0.070	0.040	0.86	0.45	0.9	15	—	−0.061
32	1708	7 Dec	160	12.3	0.089	0.067	0.044	1.21	0.42	0.3	3	—	−0.005
33	1804	7 Dec	152	13.6	0.091	0.069	0.043	1.16	0.44	−1.0	−1	—	0.002
34	1937	7 Dec	156	15.0	0.091	0.075	0.050	1.32	0.55	−0.8	−24	—	0.020
35	0000	8 Dec	166	17.2	0.095	0.078	0.055	1.82	0.81	−4.4	−82	0.85	0.030
36	0300	8 Dec	172	17.6	0.096	0.081	0.057	1.82	0.94	−4.8	−93	0.88	0.032
					Year 1977								
38	0058	14 Feb	096	16.4	0.098	0.080	0.053	1.15	0.28	—	—	—	−0.070*
39	0209	14 Feb	094	17.0	0.112	0.080	0.056	1.48	0.78	—	—	—	−0.017*
45	2048	14 Mar	086	14.1	0.090	0.078	0.054	1.43	0.58	−0.2	−2	—	0.003
46	0221	15 Mar	085	15.5	0.089	0.088	0.055	1.50	0.60	−0.1	−9	—	0.006
47	0326	15 Mar	084	14.9	0.090	0.075	0.053	1.40	0.62	−0.5	−6	—	0.005
48	1210	15 Mar	080	15.6	0.099	0.086	0.057	1.43	0.86	−0.4	−3	—	0.002
49	1537	15 Mar	076	15.6	0.101	0.090	0.056	1.66	0.93	−0.2	−3	—	0.002
51	1906	15 Mar	071	16.2	0.102	0.093	0.057	1.43	0.95	−0.2	−5	—	0.004
57	1720	23 Mar	076	16.7	0.130	0.090	0.053	1.88	0.83	0.0	—	—	−0.005*
58	1846	23 Mar	085	16.0	0.102	0.093	0.059	1.68	0.92	−0.5	—	—	0.000*
59	1939	23 Mar	083	14.2	0.099	0.088	0.052	1.71	0.90	−0.6	—	—	0.000*
60	0005	24 Mar	074	10.0	0.084	0.095	0.063	1.32	0.87	−1.1	—	—	0.007*
61	0045	24 Mar	073	10.8	0.088	0.089	0.066	1.04	0.89	−1.0	—	—	0.007*
64	1745	31 Mar	163	10.2	0.067	0.047	0.049	0.41	0.28	−3.0	—	—	0.398*
65	1847	31 Mar	168	10.9	0.074	0.054	0.051	0.95	0.32	−3.1	—	—	0.121*
89	1908	11 Nov	181	11.5	0.079	0.067	0.046	0.94	0.58	−3.8	−47	0.88	0.162
90	2011	11 Nov	204	11.4	0.104	0.110	0.047	0.97	0.62	−2.6	−32	0.85	0.104
92	1509	16 Nov	199	9.2	0.084	0.065	0.044	0.97	0.34	—	−6	—	0.033
93	1637	16 Nov	206	9.1	0.080	0.060	0.043	1.21	0.38	—	−12	—	0.053
94	0537	18 Nov	169	14.2	0.084	0.070	0.050	1.18	0.71	—	−68	—	0.082
95	0637	18 Nov	171	14.7	0.094	0.079	0.051	1.31	0.81	—	−56	—	0.052
103	1203	24 Nov	132	12.0	0.094	0.078	0.049	1.68	0.40	3.3	55	1.06	−0.067
104	1308	24 Nov	130	12.0	0.095	0.074	0.046	1.48	0.44	3.0	48	1.02	−0.071
105	1534	24 Nov	131	10.2	0.090	0.071	0.054	0.68	0.58	2.4	—	—	−0.336*
107	1234	26 Nov	074	18.5	0.121	0.087	0.059	2.10	1.15	2.4	68	1.22	−0.016
108	1338	26 Nov	080	18.9	0.108	0.078	0.055	1.50	1.12	2.6	45	0.72	−0.017
109	1439	26 Nov	079	16.6	0.140	0.083	0.056	1.12	1.15	2.4	—	—	−0.053*
110	1550	26 Nov	081	13.0	0.114	0.086	0.047	1.27	1.10	1.5	—	—	−0.054*
					Year 1978								
135	1152	9 Jan	139	13.6	0.084	0.062	0.051	1.42	0.81	−2.6	−48	1.05	0.052
136	1317	9 Jan	148	13.9	0.089	0.066	0.052	1.41	0.80	−3.5	−57	0.92	0.060
138	1650	9 Jan	148	16.4	0.097	0.069	0.053	1.72	1.02	−4.9	−96	0.94	0.046
139	1816	9 Jan	151	16.7	0.084	0.063	0.051	1.22	1.43	−5.0	−77	0.74	0.059
140	2014	9 Jan	151	17.0	0.091	0.069	0.054	1.39	1.08	−5.7	−101	0.83	0.061
141	2337	9 Jan	146	19.0	0.105	0.076	0.056	1.61	1.35	−6.6	−122	0.78	0.042
143	0138	10 Jan	150	22.0	0.112	0.094	0.062	1.79	1.62	−7.4	−170	0.85	0.032
161	1606	14 Jan	152	13.0	0.081	0.060	0.051	1.32	0.72	−4.7	−77	0.96	0.106
162	1726	14 Jan	156	12.1	0.096	0.073	0.052	1.22	0.72	−4.7	−66	0.89	0.130
163	1827	14 Jan	152	12.6	0.075	0.062	0.050	1.17	0.69	−5.0	−75	0.95	0.140
164	1942	14 Jan	148	13.8	0.086	0.064	0.052	1.38	0.70	−5.8	−81	0.78	0.087
166	0056	15 Jan	152	15.2	0.085	0.065	0.053	1.35	0.96	−6.6	−111	0.87	0.096
167	0153	15 Jan	153	15.4	0.091	0.067	0.054	1.42	1.10	−6.6	−106	0.82	0.080

TABLE 1. (*Continued*)

Run No.	Start time (GMT)	Date	Wind direction (deg T)	Wind speed U_{10} (m s^{-1})	Turbulence level σ_1/U	σ_2/U	σ_3/U	Drag coefficient 10^3C_{10}	rms wave height (m)	$T_s - T_a$ (°C)	Heat flux (W m^{-2})	10^3C_T	Stability z/L
							Year 1978						
169	0351	15 Jan	153	15.5	0.091	0.072	0.055	1.35	1.32	−6.1	−108	0.90	0.086
170	0450	15 Jan	156	17.0	0.096	0.074	0.055	1.28	1.34	−6.4	−115	0.85	0.076
175	2022	18 Jan	155	16.3	0.104	0.087	0.055	1.19	1.17	−5.2	—	—	0.078*
179	1409	26 Jan	167	14.6	0.093	0.065	0.054	0.98	0.55	−5.6	—	—	0.144*
181	1834	26 Jan	182	14.6	0.082	0.063	0.052	1.33	0.90	−7.7	—	—	0.126*
182	2010	26 Jan	180	14.1	0.088	0.066	0.055	1.42	0.89	−7.9	—	—	0.126*
190A	0946	7 Feb	075	19.4	0.105	0.093	0.058	2.20	1.19	2.4	87	1.39	−0.002
190B	1027	7 Feb	076	19.2	0.118	0.094	0.059	2.23	1.15	2.3	—	—	−0.014*
190C	1108	7 Feb	079	19.3	0.115	0.096	0.058	1.99	1.19	2.1	—	—	−0.015*
191	1224	7 Feb	075	19.5	0.120	0.096	0.058	2.15	1.35	1.7	59	1.32	−0.012

* Heat flux estimated by bulk method.

value of Garratt (1977) which is heavily influenced by data at fetches around 10 km. The extensive profile data of Kondo *et al.* (1972) at wind speeds from 7 to 20 m s^{-1}, although not included in the review, would give a result nearly identical to that of Garratt, again containing data at limited fetch.

In a direct comparison with only the beach site data of Smith and Banke (1975), who found $10^3C_{10} = 0.61 + 0.075U_{10}$, a regression on only the 38 near-neutral points from Table 1 (second line in Table 3, Fig. 6a) gives a 14% lower drag coefficient at 15 m s^{-1}. The wind speed ranges are similar. The rate of increase of the drag coefficient is 30% larger in this case than in Eq. (14).

The mean drag coefficient is lower and the wind speed dependence is the same as Eq. (14) if all runs from Tables 1 and 2 are included (Fig. 6b) and the last line in Table 3. Increased scatter and a lower correlation coefficient occur in these less uniformly selected conditions.

The drag coefficients during periods of alongshore winds are frequently much lower than during offshore or onshore winds, a result which was not anticipated. If the shoreline contains numerous sources of oil, and if surface drift is mainly with the wind, then slicks may occur more frequently at the stable platform site during periods of alongshore winds and would reduce the surface roughness by damping the shorter waves. No observation of slicks was attempted.

If a is set to 0.01 then the Charnock relation [Eq. (11)] agrees very closely with Eq. (14) at wind speeds from 8 to 13 m s^{-1}, coincides with the second line in Table 3 at $C_{10} = 1.5 \times 10^{-3}$, $U_{10} = 15$ m s^{-1}, fits the data almost as well as a regression line, and requires only one instead of two free parameters.

Some details appear consistently, however, which are not predicted by the Charnock relation. The variation of the drag coefficient with wind speed appears to be faster than predicted if the data at lower wind speeds are not included (second line in Table 2). Geostrophic departure analysis of data from hurricanes supports a continuing linear increase in the drag coefficient to extremely high wind speeds, while Eq. (11) would give a slower increase at these speeds. Large (1979) agrees closely with Eq. (14) at wind speeds from 10 to 26 m s^{-1}, but is able to distinguish a region of nearly constant C_{10} at wind speeds from 4 to 10 m s^{-1} (Table 3), a range where Kondo (1975) found capillary wave heights indicate transition from a rough to smooth surface. If the summary of Garratt (1977, Fig. 3) is viewed separately at wind speeds above 10 m s^{-1} and below 10 m s^{-1}, the same conclusion may be drawn, i.e., that the drag coefficient appears to be nearly constant at wind speeds below 10 m s^{-1} (see, also, Smith, 1967, 1974b) and to vary more rapidly, like the second line in Table 3, at the higher wind speeds.

b. Variation with sea state

A linear regression of C_{10} on rms wave height for cases of onshore winds and near-neutral stability (Table 4, Fig. 7) shows an increase with wave height but a lower correlation coefficient (0.58) than did the regression of the same drag coefficients on wind speed (Table 3). The rms wave height is not as good an indicator of the drag coefficient as wind speed, and the wave measurements do not quite reach high enough frequencies to compute a high-frequency wave height h_p as did Kondo *et al.* (1973). The drag coefficients at limited fetch are not significantly correlated with wave height (Table 4), although this negative result may be partly due to combining a

TABLE 2. Thrust anemometer data at limited fetch. The letter A indicates an alongshore wind.

Run No.	Start time (GMT)	Date	Fetch (km)	Wind direction (deg T)	Wind speed U_{10} (m s^{-1})	Turbulence level σ_1/U	σ_2/U	σ_3/U	Drag coefficient 10^3C_{10}	rms wave height h (m)	$T_s - T_a$ (°C)	Heat flux (W m^{-2})	Heat flux coefficient 10^3C_T	Stability z/L
						Year 1976								
1	1752	7 Oct	74	250	8.2	0.076	0.063	0.039	0.80	—	−0.5	6	—	−0.077
2	1158	10 Oct	A	234	16.5	0.106	0.071	0.048	1.71	—	−0.8	6	—	−0.003
7	1150	15 Oct	11	269	15.0	0.109	0.107	0.048	1.59	0.68	2.5	40	0.83	−0.028
8	1736	15 Oct	12	265	13.4	0.119	0.112	0.049	1.60	0.66	−0.8	−13	—	0.013
17	1931	21 Oct	A	232	13.5	0.099	0.076	0.051	0.64	1.07	−3.0	−22	0.42	0.079
20	1348	12 Nov	11	283	11.1	0.120	0.118	0.051	1.59	0.49	8.9	135	1.09	−0.240
22	1344	19 Nov	18	313	15.8	0.108	0.084	0.054	2.14	0.30	—	72	—	−0.029
						Year 1977								
37	1345	10 Feb	A	227	8.0	0.079	0.060	0.053	1.15	0.28	—	−9	—	0.067
41	1255	10 Mar	A	231	12.4	0.079	0.060	0.047	0.95	0.55	−2.2	−37	1.04	0.098
42	1410	10 Mar	A	230	13.8	0.076	0.062	0.048	0.73	0.60	−2.6	−37	0.81	0.104
43	1707	10 Mar	A	229	14.0	0.081	0.063	0.050	0.91	0.64	−2.9	−42	0.80	0.082
44	2008	10 Mar	A	234	11.4	0.077	0.061	0.047	0.81	0.64	−2.6	−30	0.82	0.132
52	0043	16 Mar	A	068	14.6	0.107	0.098	0.057	1.08	0.97	−0.9	−23	—	0.031
53	0146	16 Mar	A	068	13.9	0.103	0.097	0.061	0.88	0.96	−0.9	−13	—	0.026
62	0137	24 Mar	A	068	10.5	0.114	0.095	0.064	1.03	0.91	−1.0	—	—	0.006*
63	1416	24 Mar	17	018	7.8	0.100	0.091	0.080	0.97	0.83	−0.8	—	—	−0.030*
67	0451	4 Apr	13	293	19.6	0.139	0.113	0.062	1.05	0.73	−1.2	—	—	0.013*
70	1204	4 Apr	15	304	14.4	0.135	0.150	0.057	1.75	0.68	0.9	—	—	−0.018*
78	1144	6 Apr	A	223	10.2	0.079	0.078	0.049	1.17	0.74	−1.8	—	—	0.045*
79	1243	6 Apr	A	223	11.4	0.085	0.070	0.048	0.99	0.80	−2.2	—	—	0.066*
80	1546	6 Apr	A	222	12.2	0.078	0.070	0.047	0.81	0.70	−1.9	—	—	0.066*
83	0355	7 Apr	A	217	9.9	0.089	0.076	0.046	0.85	0.52	−1.0	—	—	0.005*
84	1546	1 Nov	83	246	6.5	0.085	0.057	0.036	0.69	0.17	1.1	7	0.85	−0.225
86	1311	7 Nov	17	010	10.5	0.098	0.104	0.055	1.41	0.24	3.8	54	1.03	−0.126
87	1958	7 Nov	17	025	9.5	0.109	0.116	0.050	1.95	0.29	3.2	56	1.48	−0.115
97	1207	18 Nov	203	235	13.9	0.094	0.079	0.046	1.43	0.92	—	−1	—	0.001
98	1340	18 Nov	A	230	11.8	0.100	0.069	0.047	1.43	0.84	—	7	—	−0.011
100	1706	22 Nov	15	298	6.1	0.092	0.068	0.059	0.95	0.40	−0.8	−7	—	0.168
101	1758	22 Nov	13	320	10.1	0.105	0.082	0.050	1.27	0.38	0.9	17	—	−0.062
102	1850	22 Nov	16	308	9.4	0.103	0.086	0.047	1.26	0.36	1.4	14	0.82	−0.055
112	1110	27 Nov	83	247	18.6	0.118	0.093	0.055	1.65	1.09	2.6	59	0.95	−0.021
113	1207	27 Nov	83	246	19.4	0.126	0.101	0.056	1.79	1.19	3.5	94	1.12	−0.026
115	1403	27 Nov	83	247	19.0	0.113	0.095	0.058	1.88	1.26	5.2	164	1.30	−0.044
116	1459	27 Nov	83	246	19.8	0.107	0.089	0.056	1.54	1.32	5.4	168	1.24	−0.054
117	1604	27 Nov	70	251	20.0	0.118	0.088	0.055	1.76	1.31	5.5	163	1.17	−0.041
119	1800	27 Nov	13	259	18.7	0.106	0.097	0.053	1.66	1.24	7.0	175	1.05	−0.059
120	1854	27 Nov	11	268	17.6	0.108	0.094	0.053	1.47	1.14	7.0	152	0.95	−0.074
121	2003	27 Nov	11	268	17.1	0.114	0.108	0.054	1.98	1.13	7.4	207	1.25	−0.069
124	2322	27 Nov	11	270	13.8	0.111	0.111	0.054	1.66	1.08	7.9	168	1.18	−0.139
126	0129	28 Nov	10	273	13.1	0.103	0.103	0.052	1.41	1.09	8.0	174	1.16	−0.213
						Year 1978								
133	1153	4 Jan	11	279	11.4	0.105	0.105	0.050	1.72	0.52	—	151	—	−0.230
134	1531	4 Jan	11	281	9.0	0.106	0.136	0.052	0.96	0.40	—	113	—	−0.850
145	0332	10 Jan	A	212	15.9	0.112	0.096	0.063	1.44	1.66	−4.0	−46	0.58	0.032
146	0442	10 Jan	A	226	18.2	0.132	0.102	0.062	1.45	1.47	—	3	—	−0.001
147	0921	10 Jan	A	232	17.4	0.115	0.148	0.060	1.16	1.86	—	76	—	−0.055
148	1024	10 Jan	A	232	17.4	0.109	0.111	0.057	1.24	1.68	—	82	—	−0.058
151	1334	10 Jan	A	225	17.6	0.123	0.143	0.060	1.30	1.75	—	80	—	−0.051
152	1511	10 Jan	A	231	15.8	0.114	0.128	0.059	1.27	1.80	—	89	—	−0.082
153	1739	10 Jan	A	228	17.9	0.119	0.120	0.055	1.12	1.59	—	74	—	−0.048
154	1832	10 Jan	A	230	18.4	0.123	0.098	0.053	0.74	1.62	—	86	—	−0.111
160	1952	12 Jan	11	284	11.2	0.123	0.113	0.051	1.91	0.48	—	179	—	−0.217
172	1622	15 Jan	70	251	10.8	0.103	0.093	0.054	1.20	1.42	—	51	—	−0.156
184	1520	27 Jan	A	219	13.6	0.110	0.097	0.050	0.78	1.10	−2.0	—	—	0.062*
185	1718	27 Jan	A	228	16.1	0.108	0.085	0.051	0.80	1.13	−1.3	—	—	0.025*
186	2014	27 Jan	A	226	14.8	0.112	0.094	0.048	0.99	1.12	1.0	—	—	−0.045*
187	1152	1 Feb	11	336	9.4	0.076	0.082	0.046	1.01	0.23	—	—	—	Unstable

* Heat flux estimated by bulk method.

range of fetches. The drag coefficients for alongshore winds were 30% lower but almost as well correlated with wave height as those for onshore winds.

Krugermeyer *et al.* (1978) report that the dimensionless profile slope, as measured from a mast on a surface-following buoy, increases with wave height about three times faster than the present drag coefficients (Table 4), depending somewhat on the range of heights chosen for the profile. This casts some doubt on certain earlier reports of variation of the drag coefficient with wind speed based on wind profiles, but does not affect the interpretation of eddy flux results.

c. *Variation with stability*

Because the data in the present experiment were collected primarily during periods of high wind speed the stability was small, lying in the range $-0.34 < z/L < 0.17$ with only two exceptions: run 64 in Table 1 and run 134 in Table 2. Over this range the profile equations [(6) and (8)] lead us to expect drag coefficients varying from 11% higher to 14% lower than in the neutral case, and this range of variation is comparable to the scatter in the present data.

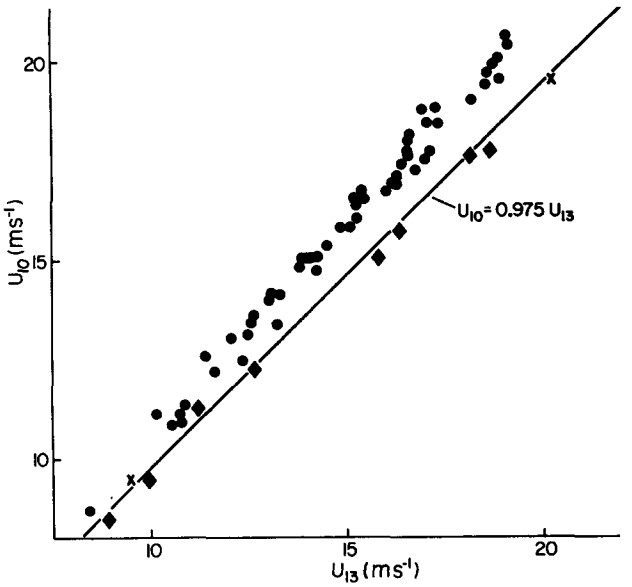

FIG. 5. Mean wind velocities U_{10} from thrust anemometers compared to simultaneous mean wind velocity U_{13} from Aerovane anemometer. Thrust 6.4 (◆) October–December 1976; thrust 6.3 (●) February 1977–January 1978; and thrust 8.1 (×) February 1978. The line $U_{10} = 0.975U_{13}$ represents calibration agreement between Aerovane and thrust anemometers.

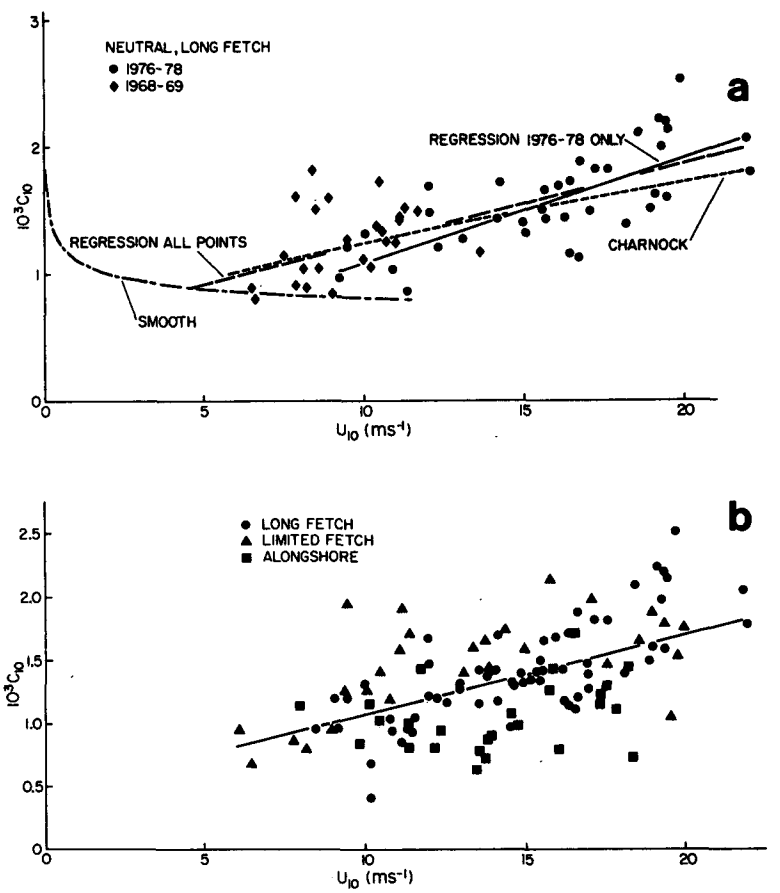

FIG. 6. Drag coefficients plotted as a function of wind speed. (a) Long fetch and neutral stability ($-0.1 < z/L < 0.05$) from Table 1 and similarly selected points from Smith (1973). Also first two regression lines from Table 3, Charnock line [Eq. (11)] and smooth line [Eq. (12)]. All points from Tables 1 and 2, and third regression line from Table 3.

TABLE 3. Regression of drag coefficient on wind speed.

Data selection	Wind speed (m s^{-1})	Number of runs	10^3C_{10} regression equation	Correlation coefficient r
Table 1, neutral, long fetch[1]	6–22	63	$0.61 + 0.063U_{10}$	0.70
Table 1, neutral, long fetch	9–22	38	$0.27 + 0.082U_{10}$	0.72
All data, Tables 1 and 2	6–22	120	$0.44 + 0.063U_{10}$	0.57
Smith and Banke (1975)	6–21	33	$0.61 + 0.075U_{10}$	0.86
Garratt (1977)	3–21	791	$0.75 + 0.067U_{10}$	
Miller (1964)	6–60		$0.75 + 0.067U_{10}$	
Large (1979)	4–10	616	1.14	
Large (1979)	10–26	975	$0.49 + 0.065U_{10}$	0.74

[1] Includes selected data from Smith (1973).

TABLE 4. Regression of neutral drag coefficient on wave height.

Data selection	rms wave height (m)	Number of runs	10^3C_{10} regression equation	Correlation coefficient r
Table 1, onshore wind	0.3–1.6	38	$1.00 + 0.69\sigma$	0.58
Table 2, offshore wind	0.3–1.3	17	$1.38 + 0.21\sigma$	0.24
Table 2, alongshore wind	0.6–1.9	15	$0.84 + 0.24\sigma$	0.50
Krugermeyer *et al.* (1978)	0.1–0.4		$1.04 + 1.57\sigma$	0.69

The measured drag coefficients have been adjusted to equivalent values at 15 m s^{-1} wind speed using the slope of the second regression line in Table 3, i.e.,

$$10^3C_{10}^{15} = 10^3C_{10} - 0.082(U_{10} - 15 \text{ m s}^{-1}). \quad (15)$$

Regression lines of C_{10}^{15} on stability (Table 5 and Fig. 8) have been fitted separately for stable and unstable stratification, omitting the two outlying cases mentioned above and also omitting runs from Table 2 with alongshore winds, some of which appear to give anomalously low drag coefficients. Although these seem to indicate good agreement with the expected variation of the drag coefficient with stability, the low correlation coefficients of the regressions indicate that while the drag coefficient varies with stability in the correct sense, quantitative agreement is probably fortuitous.

d. Variation with fetch

We might expect to find higher drag coefficients at short fetches with actively growing waves absorbing momentum from the wind than at long fetch with the waves more or less in equilibrium. The drag coefficients at long fetch in the present study are slightly lower than those in the literature (e.g., Garratt, 1977), the majority of which have been measured at limited fetch. The drag coefficients at limited fetch from Table 2 have been adjusted to remove wind speed dependence using Eq. (15), and the stability dependence has similarly been removed

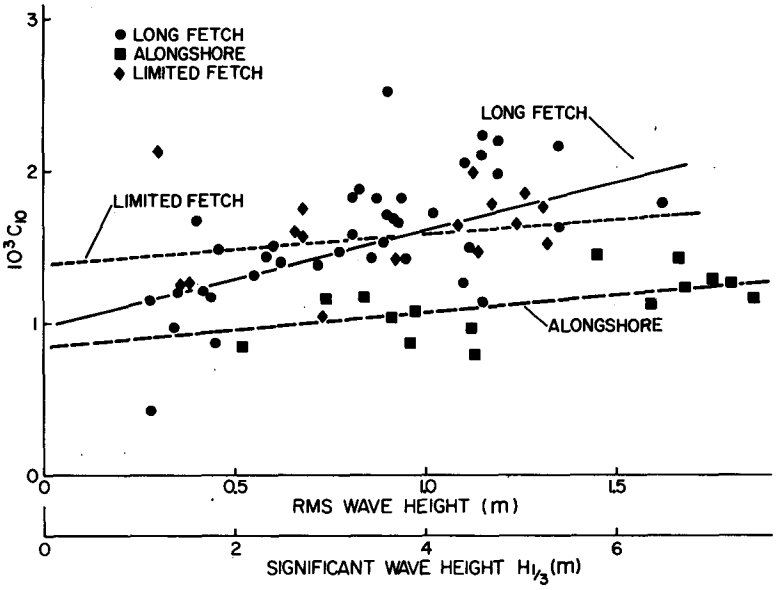

FIG. 7. Drag coefficient plotted against wave height for long-fetch alongshore, and limited fetch cases. Only runs from Tables 1 and 2 with near-neutral stability $-0.1 < z/L < 0.05$, are included. Regression lines (Table 4) are shown for the three cases.

by adding 0.6×10^{-3} z/L (unstable) or 10^{-3} z/L (stable). The neutral, 15 m s^{-1} drag coefficients plotted against dimensionless fetch Xg/U_{10}^2 do not exhibit any very strong functional dependence. Group means over ranges of multiples of 1–2, 2–5 and 5–10 have been plotted with standard errors, showing ~20% higher average values at dimensionless fetches of 500–1000 and 1000–2000 than at longer fetches. This trend is not continued at the lowest fetches, ~400. These are the highest wind speed runs and if in Eq. (15) we used a less strong wind speed dependence, then the drag coefficients would increase slightly at low fetch. Near a major harbor and two refineries, certain wind directions may on occasion produce surface slicks which reduce the wind stress and contribute to the scatter in Fig. 9. One particularly low drag coefficient (run 67) has not been used in calculating the group means. Hicks (1972) also concluded from experiments in Bass Strait and Lake Michigan that the drag coefficient does not vary noticeably with fetch.

e. *Turbulence levels*

The increase in the drag coefficient with wind speed is, as expected from similarity theory, mainly accounted for by a corresponding increase in turbulence levels, $\sigma_i/U = \overline{u_i^2}^{1/2}/U$. For the 38 runs in near-neutral stability and at long fetch (Table 1) used to derive the second line in Table 3, regression lines are

$$\sigma_1/U = 0.061 + 0.0027\ U_{10}, \quad r = 0.68, \quad (16a)$$

$$\sigma_2/U = 0.057 + 0.0017\ U_{10}, \quad r = 0.55, \quad (16b)$$

$$\sigma_3/U = 0.038 + 0.0010\ U_{10}, \quad r = 0.52. \quad (16c)$$

TABLE 5. Dependence of 15 m s^{-1} drag coefficient on stability.

	Number of runs	$10^3 C_{10}^{15}$ regression equation	Correlation coefficient r
Stable ($z/L \geq 0$)	49	$1.46 - 0.97z/L$	0.20
Unstable ($z/L < 0$)	41	$1.56 - 0.33z/L$	0.08

Between wind speeds of 10 and 20 m s^{-1} σ_1/U increases by 31% and σ_3/U by 21%, according to Eqs. (16a) and (16c). This leaves only a small increase of 5% in the downwind-vertical turbulence correlation coefficient $r_{13} = u_*(\sigma_1\sigma_3)^{-1/2}$ to account for the 75% increase in C_{10} over this wind speed range. Smith and Banke (1975) observed that vertical turbulence levels increased less rapidly than downwind levels, requiring a small and not very well resolved increase in r_{13} with wind speed to account for part of the increase in drag coefficient. The more rapid increase of downwind turbulence level with wind speed is explained by the same (40 min) averaging time including longer turbulence length scales at higher wind speeds. The downwind spectrum contributes substantial fluctuations at longer scales, while the vertical does not.

The behavior of the crosswind turbulence level [Eq. (16b)] is between that of the downwind and vertical components. The yaw motion of the platform may cause (16b) to be slightly on the high side.

SethuRaman (1979) shows a very similar dependence of σ_1 and σ_2 on U_{10} over the sea at wind speeds from 2 to 27 m s^{-1}. His empirical formulas for σ_1 and σ_2 are expressed in a different form, but agree within 15% with Eqs. (16a) and (16b) over the entire range. Turbulence levels and drag coefficients over land

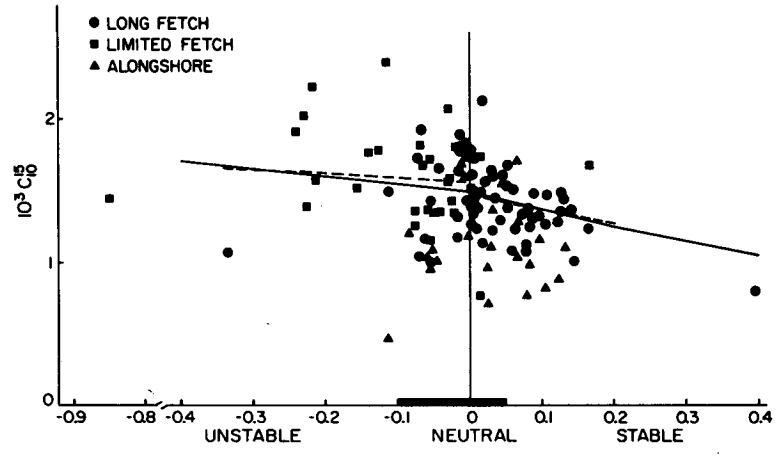

FIG. 8. Drag coefficients adjusted to 15 m s^{-1} wind speed [Eq. (15)] plotted against stability. Solid line shows expected dependence on stability from wind profile formulas and dashed lines are regressions from Table 5. The heavy part of the axis is the range $-0.1 < z/L < 0.05$ taken to be nearly neutral.

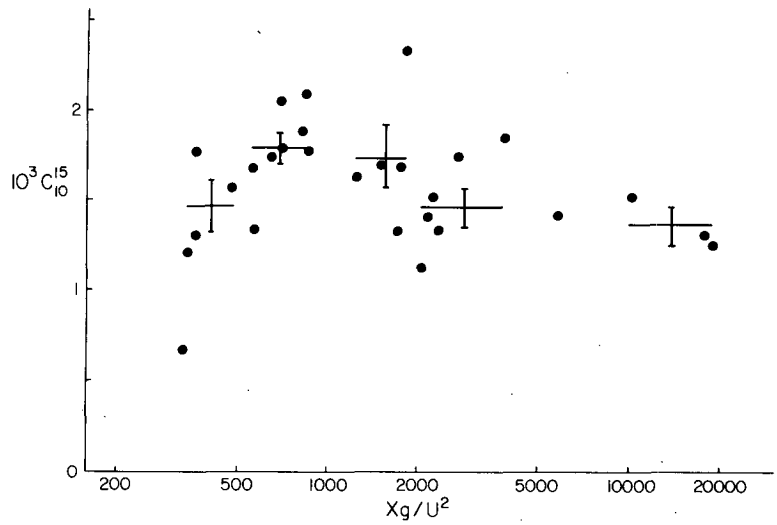

FIG. 9. Drag coefficients from Table 2 adjusted to 15 m s^{-1} wind speed and neutral stability and plotted against dimensionless fetch. Group means are shown with vertical lines giving ±standard error.

surfaces tend to be higher and do not vary with wind speed.

As has been done with the drag coefficients, it is possible to use Eq. (16) to express turbulence levels adjusted to a wind speed of 15 m s^{-1} and then to examine their stability dependence (Fig. 10). Regression lines of the 15 m s^{-1} turbulence levels on stability for 62 runs from Table 1 are (omitting runs 64 and 105 which have large values of z/L and would otherwise dominate the regression) as follows:

$$\sigma_1^{15}/U = 0.101 - 0.12\ z/L, \quad r = -0.62 \quad (17a)$$

$$\sigma_2^{15}/U = 0.084 - 0.14\ z/L, \quad r = -0.53 \quad (17b)$$

$$\sigma_3^{15}/U = 0.052 + 0.01\ z/L, \quad r = 0.14. \quad (17c)$$

The horizontal turbulence levels are correlated equally well with stability as with wind speed, and are higher in unstable conditions as one might expect. The vertical turbulence levels, on the other hand, do not appear to be significantly correlated with stability. This is a curious result since it is the vertical component of the turbulent kinetic energy which gains or loses energy from the potential energy associated with unstable or stable stratification. Large (1979) observed independently a similar variation with stability of horizontal turbulence levels and a lack of such variation of vertical turbulence levels.

Spectra of the velocity fluctuations and the wind stress cospectra were plotted in normalized form $f\phi(f)/u_*^2$ against a dimensionless frequency fz/U for neutral, stable and unstable groups. These are not reproduced here but were found to agree well with those of Large (1979), who in turn found that his spectra were similar to those of McBean (1971) measured over a flat land surface with mown grass.

4. Heat flux

The heat fluxes observed in this experiment, in which both wind speeds and sea-air temperature differences were often large, extend to much larger values than those previously available over the open ocean (Fig. 11). Regression lines of $\overline{tu_3}$ on $(T_s - T_a)U_{10}$ are given in Table 6. Two points with positive $\overline{tu_3}$ but negative $(T_s - T_a)$ (runs 1 and 2 in Table 2) have been omitted in the second and third lines in this table. The heat flux coefficient $C_T = \overline{tu_3}/(T_s - T_a)U_{10}$ may be equated to the slopes of the lines in Table 6. The intercept in the first line in Table 6 is largely a result of forcing a straight line fit to a slightly curved data set, while the intercepts in the second and third lines are small compared to the scatter of the data. For those runs in Tables 1 and 2 without direct heat flux measurements (the thermistors broke occasionally) the first line in Table 6 has been used to estimate $\overline{tu_3}$ and hence the stability.

The slope of the last line in Table 6 indicates 25% less heat flux than that reported by Smith and Banke (1975) for similar measurements over the same range of $U_{10}(T_s - T_a)$, with onshore winds passing over a coastal surf zone, while the difference in wind stress between the two sites was only 14%.

The results in Table 6 are in excellent agreement with those of Large (1979), who obtained slopes of 0.75×10^{-3} and 1.0×10^{-3} for regressions of $\overline{tu_3}$ on $(T_s - T_a)U_{10}$ in stable and unstable conditions,

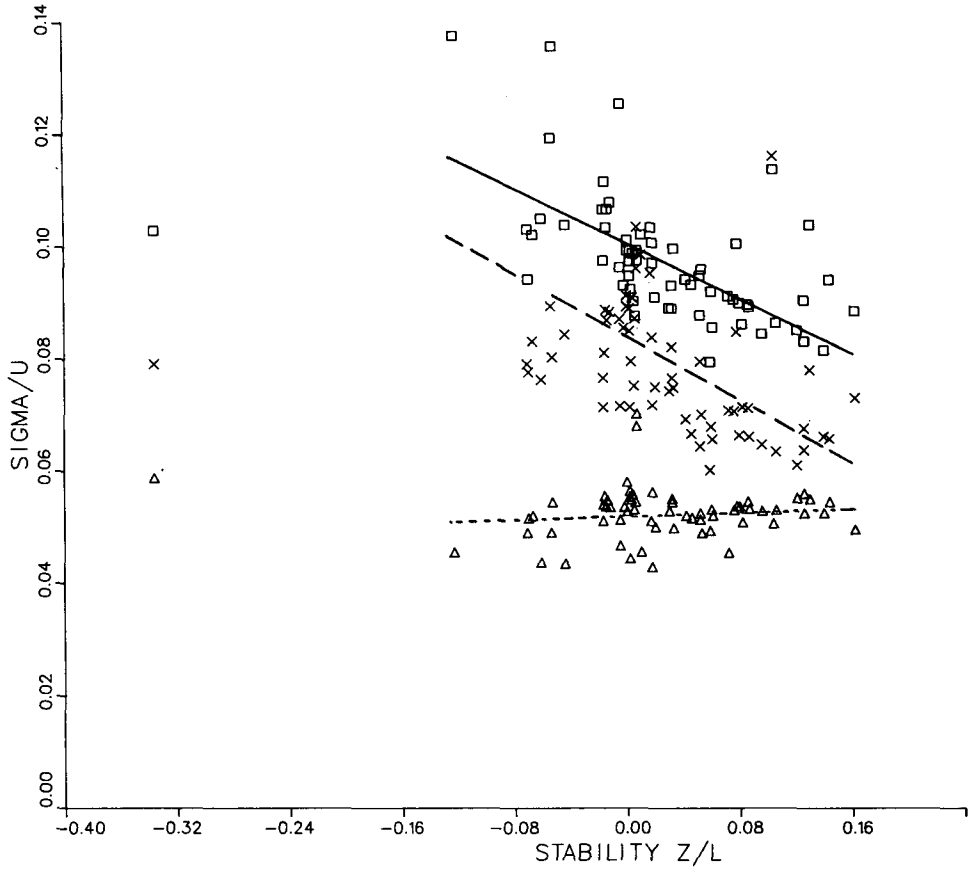

FIG. 10. Turbulence levels from Table 1 adjusted to 15 m s^{-1} wind speed [Eq. (16)] as a function of stability. Symbols are: σ_1^{15}/U (□), σ_2^{15}/U (×) and σ_3^{15}/U (△). Regression lines: solid [Eq. (17a)], dashed [(17b)] and dotted [(17c)].

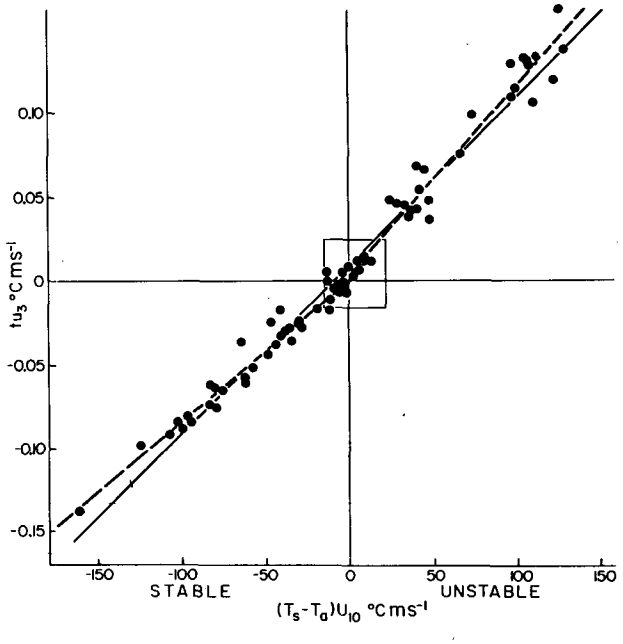

FIG. 11. Temperature flux $\overline{tu_3}$ plotted against $(T_s - T_a)U_{10}$. Regression lines from Table 6.

respectively, and then made adjustments which raised C_T slightly. Friehe and Schmitt (1976, Fig. 2) summarized available eddy correlation measurements of heat flux over the sea covering the range of the rectangle in Fig. 11, finding $10^3C_T = 0.86$ and 0.97 for stable and unstable conditions, respectively. A larger spread between stable and unstable cases in the present data is attributed to the wider range of conditions covered. If the data summarized by Friehe and Schmitt were combined with the present data, the lines in Table 6 would be essentially unchanged since the wide range of the new data would weight it heavily in the regression calculation. Francey and Garrett (1978) observed sensible heat

TABLE 6. Regression lines of heat flux on bulk parameters.

	Number of runs	$10^3\overline{tu_3}$ (°C m s^{-1}) regression equation	Correlation coefficient r
All	73	$8.7 + 0.99(T_s - T_a)U_{10}$	0.99
Stable	39	$-0.1 + 0.83(T_s - T_a)U_{10}$	0.98
Unstable	32	$3.2 + 1.10(T_s - T_a)U_{10}$	0.97

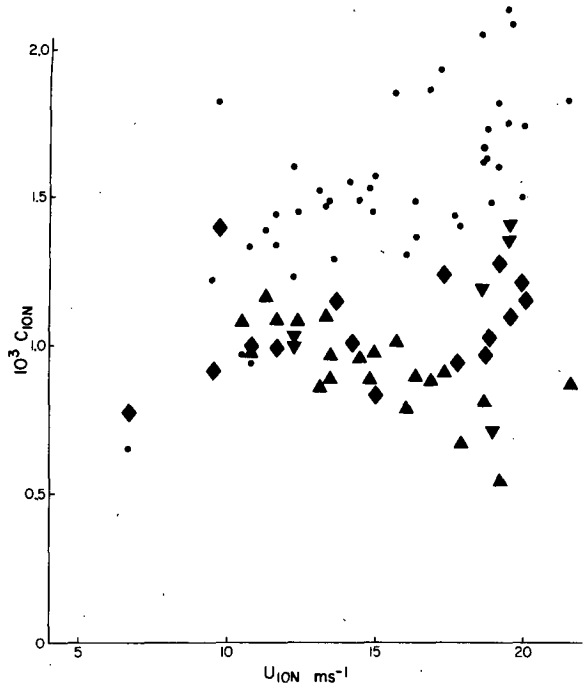

FIG. 12. Neutral heat flux coefficient C_{TN} plotted against neutral, 10 m wind speed: (▲) long fetch, stable (▼) long fetch, unstable (◆) limited fetch, unstable; (●) neutral drag coefficient C_{DN}.

exchanges exceeding 300 W m^{-2} in cold air outbreaks over subtropical waters.

Heat flux coefficients for individual data runs are listed in Tables 1 and 2 for cases in which $|T_s - T_a| > 1$°C. We cannot select data in near-neutral conditions in order to look for possible wind-speed dependence of the heat flux coefficient. Neutral heat flux coefficients C_{TN} and neutral 10 m wind speeds U_{10N} have been calculated to remove stability dependence from the data in Tables 1 and 2, using Paulson's (1970) integration of the flux-gradient relationships (Dyer, 1974); see also Large (1979). A plot of C_{TN} against U_{10N} (Fig. 12) clearly shows that the heat flux coefficient does not depend as strongly on wind speed as the neutral drag coefficient C_{DN} calculated in a similar way for the same group of data runs. The scatter in the data is such that a much smaller dependence of C_{TN} on wind speed is not disproven. (The cases of alongshore wind from Table 2, which may have been included some anomalously low drag coefficients, have not been included in Fig. 12.) This agrees with Large (1979), but contrasts with results of similar studies over shallow water (Smith and Banke, 1975; Smith *et al.*, 1976; Francey and Garratt, 1978, 1979).

Dyer (1974) gives the same stability dependence for temperature and wind profiles on the stable side, so that we might expect C_T to follow a relation similar to that given by the line in Fig. 8, while on the unstable side the stability dependence of C_T would be ~1.5 times as great as indicated by the line in Fig. 8. For modeling purposes the use of two values for $10^3 C_T$ (stable, 0.83; unstable, 1.10) may be more convenient than a pair of continuous functions of stability. A plot of C_T against stability from Tables 1 and 2 (not reproduced here) shows that two constant values of C_T fit the present data better than a smoothly varying C_T. A plot of C_{TN} (Fig. 13), on the other hand, seems to show a functional dependence (C_{TN} increases with z/L on the stable side) which should not occur if the Dyer (1974) flux-gradient relations derived over land are equally applicable over the sea. The scatter makes it difficult to draw firm conclusions. Large (1979) also notices that discrete values of C_T give the best representation of his data. In Fig. 13, C_{TN} appears to be lower in stable than in unstable cases, although this could be corrected by making the temperature profile depend more strongly on stability (e.g., Deardorff, 1968).

5. Conclusions

Wind stress and heat flux in open-sea conditions have been measured by eddy correlation methods over ranges $U_{10} = 6$–22 m s^{-1} and $U_{10}(T_s - T_a) = -160$–125°C m s^{-1}, which are larger than those previously available. As predicted by Charnock (1955) the neutral sea surface drag coefficient measured for long fetch, at wind speeds up to 22 m s^{-1}, is clearly seen to increase with increasing wind speed. The present result is slightly lower than that given by Smith and Banke (1975) or Garratt (1977). The observed drag coefficients are less closely correlated with wave height than with wind speed, and vary with stability in general agreement with profile formulas established over land.

The variability of the drag coefficient with wind speed affects not only the mean wind stress but also the transient meteorological forcing of surface water movements. For the same mean stress Eqs. (11) or (14) give ~30% higher transient forcing than a constant drag coefficient. This is a large enough difference to be of marginal importance in models of ocean movement which use observed wind velocities (e.g., Petrie and Smith, 1977), and may become significant as more precise models are developed.

The heat flux coefficient does not depend strongly on wind speed, but is larger in unstable ($C_T = 1.10 \times 10^{-3}$) than in stable ($C_T = 0.83 \times 10^{-3}$) conditions.

The above results are in agreement with those of Large (1979) at the same site. While wind stresses at even higher wind speeds are of great importance in modeling certain events such as storm surges, the present data cover a range which determines most of the mean wind stress and heat flux in most climates.

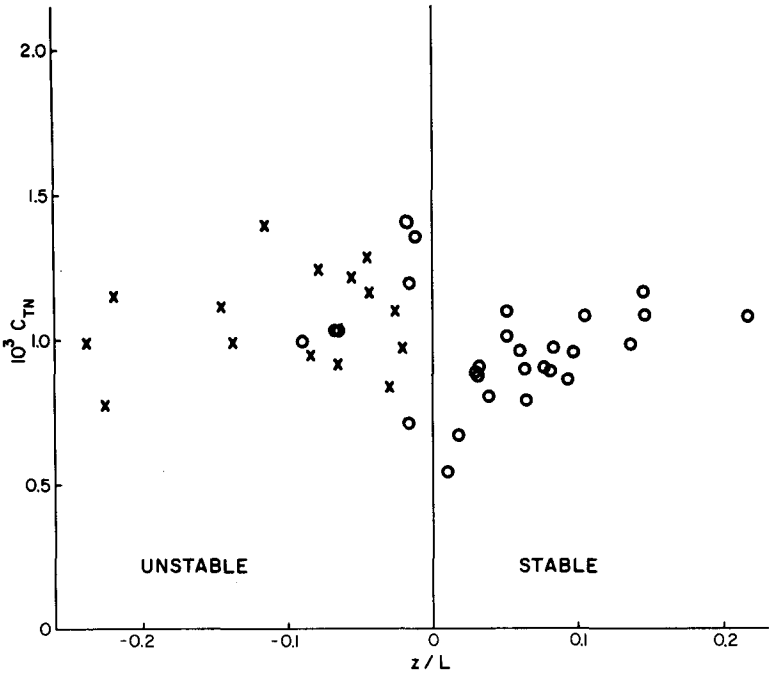

FIG. 13. Neutral heat flux coefficient C_{TN} plotted against stability z/L for long fetch (●) and limited fetch (×).

Acknowledgments. The author wishes to thank the many people at BIO whose collaboration has made this work possible. In particular, R. J. Anderson, E. G. Banke and D. L. Hendsbee have dedicated great effort to keeping the experiment running and F. W. Dobson has contributed through development of the analysis system and continuing discussions of the experiment. D. F. Dinn and R. Cassivi designed and constructed the telemetry system. The stable platform was designed by R. G. Mills of Whitman Benn and Associates Ltd. of Halifax, Nova Scotia under a contract administered by J. Brooke of BIO, and installed and maintained by Dominion Diving Ltd. of Dartmouth, Nova Scotia. The computer analysis of the data was run by M. Spencer and G. Wilson, and by R. F. Brown of Dymaxion Research Ltd., Halifax. S. Pond and W. G. Large made available both raw data and results of work in progress. N. S. Oakey made helpful comments on the manuscript. The author thanks C. S. Mason, D. L. McKeown and G. T. Needler for their support; and also L. A. E. Doe, recently retired, who initiated thrust anemometer development at BIO in 1962.

REFERENCES

Busch, N. E., 1977: Fluxes in the surface boundary layer over the sea. *Modelling and Prediction of the Upper Layers of the Ocean*, E. B. Kraus, Ed., Pergamon Press, 72–91.

Businger, J. A., 1973: Turbulent transfer in the atmospheric surface layer. *Workshop on Micrometeorology*, D. A. Haugen, Ed., Amer. Meteor. Soc., 67–100.

——, 1975: Interactions of sea and atmosphere. *Rev. Phys. Space Phys.*, **13**, 720–726 and 817–822.

Charnock, H., 1955: Wind stress on a water surface. *Quart. J. Roy. Meteor. Soc.*, **81**, 639–640.

Coulman, C. E., 1979: Air-sea transfer coefficients determined from measurements made 200 km from land. *J. Phys. Oceanogr.*, **9**, 1053–1059.

Deardorff, J. W., 1968: Dependence of air-sea transfer coefficients on bulk stability. *J. Geophys. Res.*, **73**, 2549–2557.

Dinn, D. F., 1973: A remote-controlled, multi-channel, analog-data telemetry system. Rep. No. 73-11, Bedford Institute of Oceanography, 118 pp.*

Dobson, F. W., R. F. Brown and D. R. Chang, 1974: A set of programs for analysis of time series data including fast Fourier transform spectral analysis. Rep. No. C-74-2, Bedford Institute of Oceanography, 334 pp.*

Dyer, A. J., 1974: A review of flux-profile relationships. *Bound.-Layer Meteor.*, **7**, 363–372.

Francey, R. J., and J. R. Garratt, 1978: Eddy flux measurements over the ocean and related transfer coefficients. *Bound.-Layer Meteor.*, **14**, 153–166.

——, and ——, 1979: Is an observed wind-speed dependence of AMTEX '75 heat-transfer coefficients real? *Bound.-Layer Meteor.*, **16**, 249–260.

Friehe, C. A., and K. F. Schmitt, 1976: Parameterization of air-sea interface fluxes of sensible heat and moisture by the bulk aerodynamic formulas. *J. Phys. Oceanogr.*, **6**, 801–809.

Garratt, J. R., 1977: Review of drag coefficients over oceans and continents. *Mon. Wea. Rev.*, **105**, 915–929.

Hicks, B. B., 1972: Some evaluations of drag and bulk transfer coefficients over water bodies of different sizes. *Bound.-Layer Meteor.*, **3**, 201–213.

* Available from Librarian, Bedford Institute of Oceanography, P.O. Box 1006, Dartmouth, Nova Scotia, Canada, B2Y 4A2.

Hsu, S. A., 1974: On the log-linear wind profile and the relationship between shear stress and stability characteristics over the sea. *Bound.-Layer Meteor.*, **6**, 509–514.

Kondo, J., Y. Fujinawa and G. Naito, 1973: High-frequency components of ocean waves and their relation to the aerodynamic roughness. *J. Phys. Oceanogr.*, **3**, 197–202.

——, 1975: Air-sea bulk transfer coefficients in diabatic conditions. *Bound.-Layer Meteor.*, **9**, 91–112.

Kraus, E. B., 1972: *Atmosphere-Ocean Interaction.* Oxford University Press, 275 pp.

Krugermeyer, L., M. Gruenwald and M. Dunckel, 1978: The influence of sea waves on the wind profile. *Bound.-Layer Meteor.*, **14**, 403–414.

Large, W. G., 1979: The turbulent fluxes of momentum and sensible heat over the open sea during moderate to strong winds. Ph.D. thesis, Dept. of Physics and Institute of Oceanography, University of British Columbia, 180 pp.

McBean, G. A., 1971: The variations of the statistics of wind, temperature and humidity fluctuations with stability. *Bound.-Layer Meteor.*, **1**, 438–457.

Miller, B. I., 1964: A study of the filling of Hurricane Donna (1960) over land. *Mon. Wea. Rev.*, **92**, 389–406.

Paulson, C. A., 1970: The mathematical representation of wind speed and temperature profiles in the unstable atmospheric surface layer. *J. Appl. Meteor.*, **9**, 857–861.

Petrie, B., and P. C. Smith, 1977: Low-frequency motions on the Scotian shelf and slope. *Atmosphere*, **15**, 117–140.

Pond, S., 1968: Some effects of buoy motion on measurements of wind speed and stress. *J. Geophys. Res.*, **73**, 507–512.

——, G. T. Phelps, J. E. Paquin, G. McBean and R. W. Stewart, 1971: Measurements of the turbulent fluxes of momentum, moisture and sensible heat over the ocean. *J. Atmos. Sci.*, **28**, 901–917.

——, and W. G. Large, 1978: A system for remote measurements of air-sea fluxes of momentum heat and moisture during moderate to strong winds. Ms. Rep. No. 32, Institute of Oceanography, University of British Columbia, 55 pp.

SethuRaman, S., 1979: Structure of turbulence over water during high winds. *J. Appl. Meteor.*, **18**, 324–328.

Smith, S. D., 1967: Thrust-anemometer measurements of wind-velocity spectra and of Reynolds stress over a coastal inlet. *J. Mar. Res.*, **25**, 239–262.

——, 1973: Thrust anemometer measurements over the sea re-examined. Rep. No. 73-1, Bedford Institute of Oceanography, 23 pp.*

——, 1974a: Program A to D for analog-to-digital conversion and processing of time series data. Rep. No. C-74-1, Bedford Institute of Oceanography, 68 pp.*

——, 1974b: Eddy flux measurements over Lake Ontario. *Bound.-Layer Meteor.*, **6**, 235–255.

——, 1978: Eddy fluxes of momentum and heat measured over the Atlantic Ocean in gale force winds. *Turbulent Fluxes through the Sea Surface, Wave Dynamics and Prediction*, A. Favre and K. Hasselmann, Eds., Plenum Publishing Corp., 35–50.

——, 1980: Dynamic anemometers. *Instruments and Methods in Air-Sea Interaction*, F. W. Dobson, L. Hasse and R. Davis, Eds., Plenum Publishing Corp., 65–80.

——, and E. G. Banke, 1975: Variation of the sea surface drag coefficient with wind speed. *Quart. J. Roy. Meteor. Soc.*, **101**, 655–673.

——, R. J. Anderson, E. G. Banke, E. P. Jones, S. Pond and W. G. Large, 1976: A comparison of the air sea interaction flux measurement systems of the Bedford Institute of Oceanography and the Institute of Oceanography, University of British Columbia. Rep. No. 76-17, Bedford Institute of Oceanography, 41 pp.*

Stewart, R. W., 1961: Wind stress on water. *Proc. Symposium on Mathematical Hydrodynamical Models of Physical Oceanography*, Institut for Meereskunde, University of Hamburg, Germany, 399–408.

——, 1967: Mechanics of the air-sea interface. *Phys. Fluids*, **10**, S47–S55.

——, 1974: The air-sea momentum exchange. *Bound.-Layer Meteor.*, **6**, 151–167.

Wu, J., 1969: Froude number scaling of wind-stress coefficients. *J. Atmos. Sci.*, **26**, 408–413.